ELSEVIER

Journal of Organometallic Chemistry 640 (2001) 57–64

Journal of Organometallic Chemistry

www.elsevier.com/locate/jorganchem

Synthesis and circular dichroism spectra of silver(I) complexes with *R*,*R*-DIOP (4*R*,5*R*-*trans*-4,5-bis[(diphenylphosphino)methyl]-2,2-dimethyl-1,3-dioxalane): crystal structures of $[AgCl(R,R\text{-DIOP})]_2 \cdot 2CHCl_3$, $\{[AgBr(R,R\text{-DIOP})]_2\}_2 \cdot CH_2Cl_2 \cdot 2H_2O$, $[AgI(R,R\text{-DIOP})]_2$ and $[AgSCN(R,R\text{-DIOP})]_2$

Biao Wu [a,b], Xin-Tao Wu [b], Xuan Tian [c], Wen-Hua Sun [a,*]

[a] *State Key Laboratory of Engineering Plastics and Center for Molecule Sciences, Institute of Chemistry, Chinese Academy of Sciences, Beijing 100080, People's Republic of China*

[b] *State Key Laboratory of Structural Chemistry, Fujian Institute of Research on the Structure of Matter, Chinese Academy of Sciences, Fuzhou, Fujian 350002, People's Republic of China*

[c] *National Laboratory of Applied Organic Chemistry, Lanzhou University, Lanzhou 730000, People's Republic of China*

Received 11 May 2001; accepted 28 July 2001

Abstract

The title silver(I) complexes as $[AgX(R,R\text{-DIOP})]_2$ dimers (X = Cl, Br, I or SCN) were synthesized either by the reaction of $[Ag(NO_3)(R,R\text{-DIOP})]_n$ with NaX or the reaction of AgX with *R*,*R*-DIOP. The complexes were confirmed by elemental analysis, IR, ^{1}H- and ^{31}P-NMR, UV–vis and circular dichroism (CD) spectra, as well as single-crystal X-ray characterization. X-ray analysis showed that the silver atoms are tetrahedral, surrounded by two bridged halides and two phosphorus atoms of the bridged *R*,*R*-DIOP ligands. The Ag···Ag distances, ranging from 3.065(6) to 3.724(1) Å, are dependent on the polarizability of the halide anions. All of the solid-state structures of the complexes are crystallized in triclinic, space group *P*1 (no. 1). The CD spectra of these complexes demonstrate their chirality, and their Cotton effects vary according to the different halides, i.e. a negative band (at 241 nm) for **1** (X = Cl), a positive one for **2** (X = Br) and **3** (X = I), and a strong positive band for **4** (X = SCN).

Keywords: Silver complexes; *R*,*R*-DIOP; CD spectra; Cotton effect; Structures

---

1. Introduction

The chiral ligand *R*,*R*-DIOP (4*R*,5*R*-*trans*-4,5-bis[(diphenylphosphino) - methyl] - 2,2 - dimethyl - 1,3-dioxalane), first synthesized by Dang and Kagan [1], has been extensively studied for asymmetric catalytic reactions [2–4]. Numerous complexes of rhodium, ruthenium, cobalt and platinum have been reported, and their well-defined structures revealed that the DIOP ligand acted as a chelate ligand [5]. On the contrary, the copper and silver complexes were rarely reported, perhaps owing to their poor catalytic properties [6]. However, copper(I) and silver coordination chemistry has attracted great attention because it is a very important part of metal-directed current supramolecular self-assembly chemistry [7], and it could create some interesting coordination environments [8]. It was reported that these metal complexes, when coordinated with heteroatom ligands, have been assembled to form some striking structures, for instance, molecular cavities and macrocyclic frameworks [9]. Moreover, some silver–phosphine complexes were reported to have antitumor activities [10] and luminescent properties [11]; recently, there was a report of a silver–phosphine complex catalyzing the enantioselective addition [12].

Previously, the reaction of silver nitrate with *R*,*R*-DIOP was carried out to give a helical infinite chain

---

* Corresponding author.

E-mail address: whsun@infoc3.icas.ac.cn (W.-H. Sun).

PII: S0022-328X(01)01171-8

[13]. In the present case, reactions of $[Ag(NO_3)(R,R\text{-DIOP})]_n$ with NaX and/or AgX with *R*,*R*-DIOP occurred to form their corresponding dimer complexes $[AgX(R,R\text{-DIOP})]_2$, in which the two DIOP ligands linked two silver atoms, along with the two bridged halides. Herein, we report the syntheses and characterization of the dimer complexes $[AgX(R,R\text{-DIOP})]_2$ (X = Cl, Br, I and SCN), along with their circular dichroism (CD) spectra.

2. Experimental

All reactions were completed under a positive pressure of pure argon (Ar) using standard Schlenk techniques, in a dark environment (aluminum foil). The solvents were dried and deoxygenated prior to use. The optically pure phosphine ligand *R*,*R*-DIOP was prepared from L-tartaric acid according to a previous literature report [14]. $[AgNO_3(R,R\text{-DIOP})]_n$ was synthesized as reported by Wu et al. [13]. Elemental analyses were carried out in a Carlo–Erba 1106 microanalyzer. The ^{1}H- and ^{31}P-NMR spectra were recorded at 500 and 202 MHz, respectively, in a Brucker AM NMR spectrometer with corresponding standards of internal TMS and external H_3PO_4. IR spectra were recorded as KBr discs in a Perkin–Elmer 577 spectrometer. UV–vis spectra were obtained in a Shimadzu UV-3000 spectrophotometer in the region of 200–700 nm. CD spectra were recorded in a JASCO-20C Automatic Recording spectropolarimeter, testing the characteristic electronic absorption of the complexes from 220 to 300 nm.

The title complexes could be easily synthesized by the reaction of NaX and $[AgNO_3(R,R\text{-DIOP})]_n$ in CH_2Cl_2. The mixture of NaX (X = Cl, Br, I or SCN, 0.30 mmol) and $[AgNO_3(R,R\text{-DIOP})]_n$ (0.14 g, 0.20 mmol) was refluxed in CH_2Cl_2 (10 ml) for 10 min and cooled to room temperature. The precipitate was filtered off and washed with CH_2Cl_2 (3 × 5 ml). The filtrate was concentrated in vacuum to ca. 5 ml and Et_2O (10 ml) was added to afford a white powder. The resulting white powder was collected and washed with Et_2O to give the title complexes in moderate yields (40–60%) after drying in vacuum. In this procedure, however, it was difficult to control the reaction conditions to obtain good yields with reproducibility.

Interestingly, the reaction of fresh AgX and *R*,*R*-DIOP in CH_2Cl_2 under reflux provided the title complexes in high yields. In this procedure, AgX was prepared just prior to use. After refluxing the mixture of AgX (0.3 mmol) and *R*,*R*-DIOP (0.10 g, 0.20 mmol) in CH_2Cl_2 (10 ml) for 10 min, the corresponding products were purified and collected as mentioned above. $[AgCl(R,R\text{-DIOP})]_2$ (**1**) was isolated to afford 0.10 g (78.1%). Anal. Calc. for $C_{31}H_{32}Ag_1Cl_1O_2P_2$: C, 58.01; H, 5.03; P, 9.65. Found: C, 57.89; H, 4.97; P, 9.55%. IR (KBr disc): 1435.1(s), 1352.0(s), 1176.4(m), 874.4(s) and 561.5(s) cm^{-1}. ^{1}H-NMR ($CDCl_3$, TMS): 0.88 (s, 6H, $(CH_3)_2C$), 2.75 (m, 2H, CH_2P), 3.03 (m, 2H, CH_2P), 4.91 (br, 2H, 2C*H*), 7.34–7.47 (m, 20H, *Ph*) ppm. ^{31}P-NMR ($CDCl_3$, H_3PO_4): +31.88 (br, d, $^1J_{Ag-P}$ = ca. 713 Hz) ppm.

$[AgBr(R,R\text{-DIOP})]_2$ (**2**) was isolated to yield 0.12 g (87.6%). Anal. Calc. for $C_{31}H_{32}Ag_1Br_1O_2P_2$: C, 54.25; H, 4.70; P, 9.65. Found: C, 54.00; H, 4.76; P, 9.47%. IR (KBr disc): 1434.7(s), 1370.9(s), 1163.3(m), 822.1(s) and 507.0(s) cm^{-1}. ^{1}H-NMR ($CDCl_3$, TMS): 0.87 (s, 6H, $(CH_3)_2C$), 2.78 (m, 2H, CH_2P), 3.04 (m, 2H, CH_2P), 4.92 (br, 2H, C*H*), 7.25–7.47 (m, 20H, *Ph*) ppm. ^{31}P-NMR ($CDCl_3$, H_3PO_4): −8.551 (br, s) ppm.

$[AgI(R,R\text{-DIOP})]_2$ (**3**) was isolated to afford 0.13 g (88.8%). Anal. Calc. for $C_{31}H_{32}Ag_1I_1O_2P_2$: C, 50.78; H, 4.40; P, 8.45. Found: C, 51.51; H. 4.66; P, 8.55%. IR (KBr disc): 1431.4(s), 1360.0(s), 1157.6(m), 853.6(s) and 496.5(s) cm^{-1}. ^{1}H-NMR ($CDCl_3$, TMS): 0.88 (s, 6H, $(CH_3)_2C$), 2.75 (m, 2H, CH_2P), 3.03 (m, 2H, CH_2P), 4.90 (br, 2H, C*H*), 7.22–7.43 (m, 20H, *Ph*) ppm. ^{31}P-NMR ($CDCl_3$, H_3PO_4): −13.302 (br, s) ppm.

$[Ag(SCN)Br(R,R\text{-DIOP})]_2$ (**4**) was isolated to yield 0.12 g (90.5%). Anal. Calc. for $C_{32}H_{32}Ag_1N_1O_2P_2S_1$: C, 57.84; H, 4.85; P, 9.32. Found: C, 57.80; H. 4.65; P, 9.28%. IR (KBr disc): 2070.0(s), 1435.4(s), 1090.1(m), 803.3(s) and 510.1(s) cm^{-1}. ^{1}H-NMR ($CDCl_3$, TMS): 0.906 (s, 6H, $(CH_3)_2C$), 2.757 (m, 2H, CH_2P), 3.045 (m, 2H, CH_2P), 4.892 (br, 2H, C*H*), 7.291–7.455 (m, 20H, *Ph*) ppm. ^{31}P-NMR ($CDCl_3$, H_3PO_4): +31.34 (br, d, $^1J_{Ag,P}$ = ca. 214 Hz) ppm.

2.1. X-ray crystallographic study

The colorless crystals of complexes **1**, **3** and **4** were obtained by the slow evaporation of their $CHCl_3$ solutions, and of complex **2** from its CH_2Cl_2 solution. All data were collected in a Siemens SMART CCD area-detector diffractometer using Mo–K$_\alpha$ radiation (λ = 0.71073 Å). A total of 1261 frames were collected for each complex with a graphite monochromator in a three-cycle goniometer (fixed χ axis). The exposure time of one frame was 10 s. The data were reduced by SIANT [14] and corrected for absorption by SADABS [15] with maximum absorption corrections of 1.000 and minimum corrections of 0.822 (**1**), 0.453 (**2**), 0.716 (**3**), and 0.233 (**4**), respectively. All the complexes were crystallized in the triclinic, $P1$ space group, and the crystal data are given in Table 1.

2.2. Structure analysis and refinement

Complex **1**: the heavy atoms were solved using the direct method. The remaining atoms were located in successive difference Fourier syntheses. The structure was refined using a full-matrix least-squares technique. All non-hydrogen atoms were refined with anisotropic thermal parameters. Only hydrogen atoms on chiral carbon atoms were calculated, using a riding model and including the structure factor calculation. The final $R = 0.0571$, $wR = 0.1603$ for 689 parameters and 5619 reflections with $I \geq 2\sigma(I)$; maximum residual electron density = 1.557 e Å^{-3} around the chlorine atom of the solvent CH_2Cl_2. Weighting scheme: $w = 1/[\sigma^2(F_o^2) + (0.1153P)^2 + 3.5221P]$ where $P = (F_o^2 + 2F_c^2)/3$.

Complex **2** was analyzed similarly, to give a final $R = 0.0538$, $wR = 0.1513$ for 1288 parameters and 13 293 reflections with $I \geq 2\sigma(I)$. The maximum residual electron density is 1.064 e Å^{-3}. Weighting scheme: $w = 1/[\sigma^2(F_o^2) + (0.1174P)^2$ where $P = (F_o^2 + 2F_c^2)/3$.

Complex **3** was calculated using an analogous method, with some carbon atoms of the phenyl group restrained as planes, to give a final $R = 0.0338$, $wR = 0.1007$ for 667 parameters and 6389 reflections with $I \geq 2\sigma(I)$; maximum residual electron density = 0.675 e Å^{-3}. Weighting scheme: $w = 1/[\sigma^2(F_o^2) + (0.0481P)^2]$ where $P = (F_o^2 + 2F_c^2)/3$.

Complex **4** was analyzed similarly to complex **3**, with all carbon atoms of the phenyl group restrained as planes, to give a final $R = 0.0801$, $wR = 0.2141$ for 463 parameters and 5340 reflections with $I \geq 2\sigma(I)$; maximum residual electron density = 0.735 e Å^{-3}. Weighting scheme: $w = 1/[\sigma^2(F_o^2) + (0.1454P)^2 + 7.2371P]$ where $P = (F_o^2 + 2F_c^2)/3$.

The absolute configuration of all complexes was confirmed by an χ refinement [16]. All calculations were performed in an INDY workstation using the SHELXL-93 program package [15].

3. Results and discussion

$[AgNO_3(R,R\text{-DIOP})]_n$ were reacted with sodium halides NaX (X = Cl, Br, I, or SCN) to form the title complexes. The nitrate anion was exchanged by the halide due to the silver-affinity of halides. Moreover, the original helical chain of $[AgNO_3(R,R\text{-DIOP})]_n$ was broken to form its corresponding dimer complex with the assistance of two bridged halides. The complexes were formed in various yields by changing the reaction conditions, with a by-product observed as a precipitate in the reaction. The different conditions affected the nitrate–halide exchange, potentially forming different species beyond the title product.

Table 1
Crystal data and structure refinement parameters for complexes **1**–**4**

Complex	1	2	3	4
Empirical formula	$C_{64}H_{66}Ag_2Cl_8O_4P_4$	$C_{125}H_{134}Ag_4Br_4Cl_2O_{10}P_8$	$C_{62}H_{64}Ag_2I_2O_4P_4$	$C_{64}H_{64}Ag_2N_2O_4P_4S_2$
Formula weight	1522.39	2866.10	1466.55	1326.90
Temperature (K)	293(2)	293(2)	293(2)	293(2)
Wavelength (Å)	0.71073	0.71073	0.71073	0.71073
Crystal system	Triclinic	Triclinic	Triclinic	Triclinic
Space group	P1	P1	P1	P1
Unit cell dimensions				
a (Å)	10.4559(1)	14.329(2)	10.3148(2)	10.6519(9)
b (Å)	13.6746(2)	15.579(2)	12.7360(3)	12.5609(10)
c (Å)	14.0125(2)	16.674(3)	12.7519(2)	12.7575(10)
α (°)	110.836(1)	106.716(10)	65.270(1)	65.855(2)
β (°)	104.836(1)	91.14(2)	88.294(1)	82.981(2)
γ (°)	98.064(1)	113.294(14)	84.987(1)	86.158(2)
V (Å^3)	1749.89(4)	3236.2(8)	1515.71(5)	1545.6(2)
Z	1	1	1	1
μ (mm^{-1})	1.000	2.025	1.815	0.852
D_{calc} (g cm^{-3})	1.445	1.471	1.607	1.426
F(000)	772	1446	728	678
h	−8–11	−17–16	−12–12	−12–12
k	−15–15	−18–14	−11–15	−9–14
l	−15–13	−19–19	−7–15	−15–15
Dimension	0.43, 0.30, 0.25	0.25, 0.22, 0.15	0.50, 0.44, 0.40	0.25, 0.23, 0.17
R_{int}	0.0149	0.0242	0.0162	0.0806
R_σ	0.0358	0.0651	0.0355	0.0541
R [a]	0.0571	0.0538	0.0339	0.0801
wR [b]	0.1603	0.1513	0.1029	0.2141
Goodness-of-fit	1.064	1.010	1.156	1.069
χ	0.00(5)	0.031(12)	0.02(2)	0.05(7)

[a] $R = \Sigma \| F_o | - | F_c \| / \Sigma | F_o |$.

[b] $wR = [\Sigma w(|F_o| - |F_c|)^2 / \Sigma w |F_o|^2]^{1/2}$.

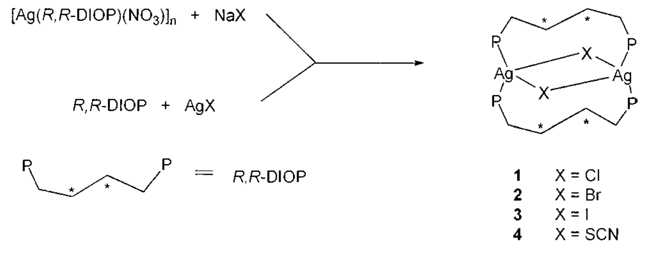

Scheme 1.

Table 2
Band maxima λ_{max} (nm), extinction coefficients (dm^3 cm^{-1} mol^{-1}) in the UV–vis spectra; band maxima λ_{max} (nm), the difference in the extinction coefficients for left- and right-handed circularly polarized light ε (dm^3 cm^{-1} mol^{-1}) in CD spectra of complexes **1**–**4** (in CH_2Cl_2)

Complex	UV–vis, λ_{max} ($\varepsilon_{mol} \times 10^{-4}$)	CD, λ_{max} ($\Delta\varepsilon$)
1	241 (1.35)	247 (−6.46)
2	258 (1.15)	236 (−3.65), 252 (+4.65), 272 (−1.66)
3	235 (1.87)	232 (−4.26), 269 (+6.39)
4	232 (2.69)	224 (−12.64), 246 (−3.73), 267 (+15.51)

However, the reaction of AgX with *R*,*R*-DIOP gave a stable yield of the corresponding complexes. The silver halide was easily prepared from the stoichiometric reaction of $AgNO_3$ and sodium halide. The fresh AgX was added into a CH_2Cl_2 solution of *R*,*R*-DIOP. Driven by the formation of the highly soluble complex in CH_2Cl_2, the amount of AgX was reduced by reacting with *R*,*R*-DIOP. In general, an excess amount of AgX was used on the basis of the easy synthesis of AgX, but more steps are involved in the synthesis of *R*,*R*-DIOP. In this case, the title complex could be easily separated. All AgX was consumed upon increasing the amount of *R*,*R*-DIOP to a slight excess, but removal of *R*,*R*-DIOP from the corresponding title products was impossible.

The synthesis of the title complexes is shown in Scheme 1. The complexes are soluble in CH_3OH, CH_2Cl_2, $CHCl_3$, CH_3CN, and DMF, but insoluble in EtOH, Et_2O and petroleum ether. The complexes were confirmed by satisfactory elemental analyses. They are relatively stable under Ar atmosphere, but the colorless transparent solutions and white powders could turn slightly gray in air, especially their solutions. All the complexes showed similar IR spectra except for a very strong band at 2070 cm^{-1} in complex **4**, which is assigned to the characteristic absorption band of terminal SCN in a bridged silver complex [17]. ^{1}H-NMR measurement also showed characteristic spectra of the complexes.

The UV–vis absorption and CD spectra of the complexes were measured at room temperature. In CH_2Cl_2, an intense UV absorption is found at 241 nm with $\varepsilon_{max} = 1.35 \times 10^4$ dm^3 mol^{-1} cm^{-1} for **1**, the absorption band is broadened for complex **2**, while shoulder-like absorptions appear for complexes **3** and **4**. The former band is due to the absorbency of the free ligand, whereas the shoulder band was assigned to the metal-to-ligand charge transfer (MLCT) according to a previous study [11]. As expected, the hypochromic shift of the 241 nm transition and the appearance of a shoulder-like band from complexes **1**–**4** is due to the polarizability of halide ions increasing from Cl to Br, I and S (in SCN), respectively. At room temperature, the CD spectra of complexes **1**–**4** display their chirality and the evident Cotton effects. A negative Cotton effect at 247 nm with $\Delta\varepsilon_{247} = -6.46$ dm^3 mol^{-1} cm^{-1} is shown in the spectrum of complex **1**. For complex **2**, an additional positive band is shown at 252 nm with $\Delta\varepsilon_{252} = +4.65$ dm^3 mol^{-1} cm^{-1}, while for complex **3** the positive Cotton effect increases and the negative one decreases. For complex **4**, the CD spectrum displays a very large positive Cotton effect. This also shows the relationship between the Cotton effect of the complexes with the polarizability of halide ions. The band maximums and their intensities in the UV–vis and CD spectra of **1**–**4** are summarized in Table 2.

To determine the structures of the title complexes, single-crystal X-ray diffraction was used to obtain their absolute structures. The crystal structures of the title complexes are built from well-separated discrete molecules with no crystallographically imposed symmetry. Figs. 1–4 show the perspective views of the structures of $[AgCl(R,R\text{-DIOP})]_2{\cdot}2CHCl_3$ (**1**), $\{[AgBr(R,R\text{-DIOP})]_2\}_2{\cdot}CH_2Cl_2{\cdot}2H_2O$ (**2**), $[AgI(R,R\text{-DIOP})]_2$ (**3**) and $[AgSCN(R,R\text{-DIOP})]_2$ (**4**), respectively. The complexes contain binuclear units in which the metal is coordinated to two P atoms and two halide ions (i.e. Cl, Br, I and S (for SCN), respectively) in a distorted arrangement; which is different from a normal tetrahedron such as $[Ag(py)_4]ClO_4$ (N–Ag–N, 110.2(2)°) [18]. The molecule 4*R*,5*R*-*trans*-4,5-bis[(diphenylphosphino)-methyl]-2,2-dimethyl-1,3-dioxalane (*R*,*R*-DIOP) acts as a bridged ligand with the two P atoms coordinating to different Ag atoms. The selected bonds and angles for complexes **1**–**4** are collected in Tables 3–6, respectively. The feature of the title complexes is a double-ring structure: the outer ring consists of an Ag–DIOP–Ag–DIOP 14-membered ring in which C(2), C(3), C(9) and C(10) are chiral carbon atoms with *R* absolute configuration, while the inner ring consists of the two halide anions and silver atoms, forming a four-membered ring. Both silver atoms are also linked by the halide anions (or the sulfur atom of the SCN complex) so that the cores of the complexes are approximate rhomboids with Ag···Ag and X···X diagonals.

These four atoms are coplanar (deviations are less than 0.03 Å). The four P atoms are coplanar (deviations less than 0.03 Å), with the metals also located in this plane (deviations are less than 0.03 Å) for the four complexes. The intersecting angles (°) of these two planes are 73.9 (complex **1**), 102.0 (complex **2**), 98.4 (complex **3**) and 87.7 (complex **4**). The structures of the four complexes are distinguishable from that of $[AgNO_3(R,R\text{-DIOP})]_n$, which is a right-handed helical infinite chain [13]. In these cases, *R*,*R*-DIOP bridged two metal centers; however, it was common for *R*,*R*-DIOP to form a seven-membered heterometallic ring with other transition metals, such as Ru, Rh, Pt, Pd and Ni [5].

The selected bond lengths and angles for complex **1** are given in Table 3. In this complex, the coordination polyhedron around Ag(1) differs slightly from that around Ag(2), as the angles P(1)–Ag(1)–P(2) and P(3)–Ag(2)–P(4) are, respectively, 130.71(4) and 133.61(4)°, which are larger than the corresponding 124.4(1) and 128.6(1)° found in $(AgClP_2C_{29}H_{30})_2$ [19]. The Ag–P bond distances are 2.427(4)–2.490(5) Å. The Ag–Cl distances, 2.649(4)–2.703(4) Å (average 2.677(4) Å) agree well with the mean Ag–Cl distances (2.668(2) Å) of $(AgClP_2C_{36}H_{30})_2$ [20].

In complex **2**, two similar molecules are arranged differently in a unit with the torsion angle of

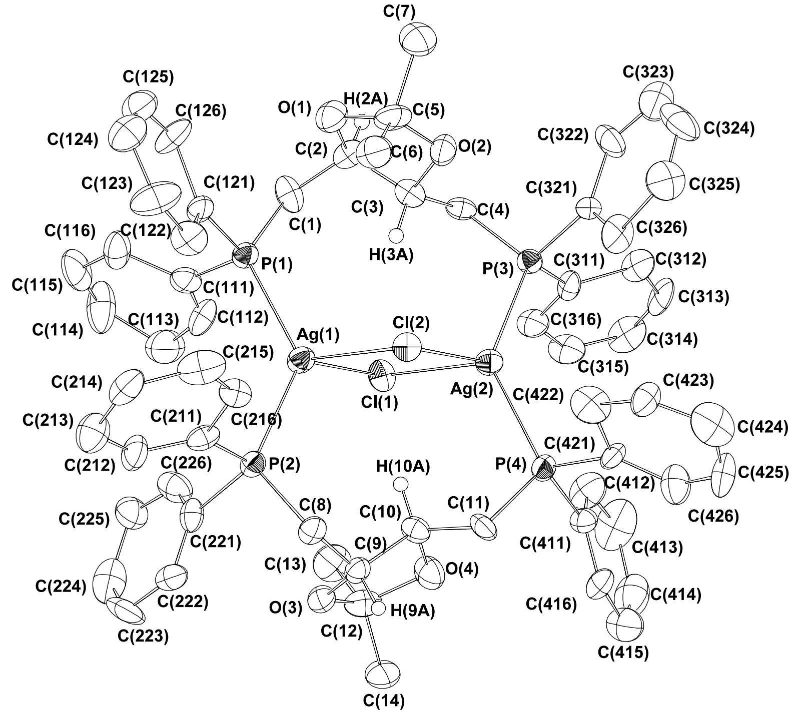

Fig. 1. Perspective view of $[AgCl(R,R\text{-DIOP})]_2$ at the 30% probability level. Some hydrogen atoms and solvents are omitted for clarity.

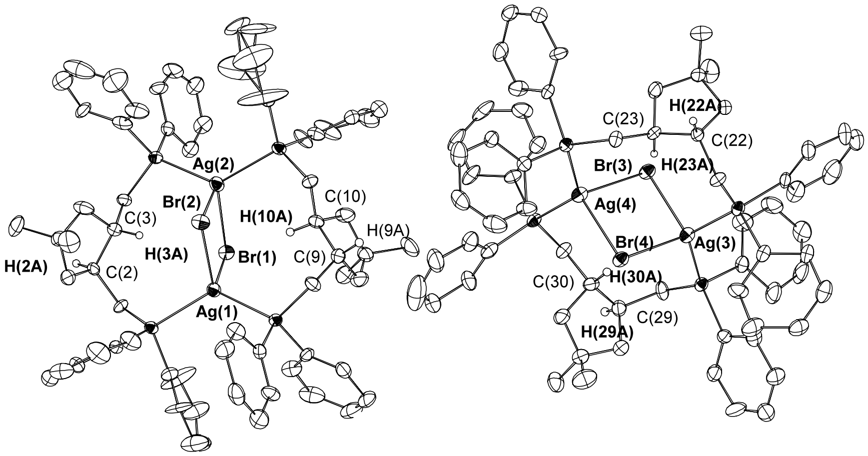

Fig. 2. Perspective view of $\{[AgBr(R,R\text{-DIOP})]_2\}_2$ at the 30% probability level. Some hydrogen atoms and solvents are omitted for clarity.

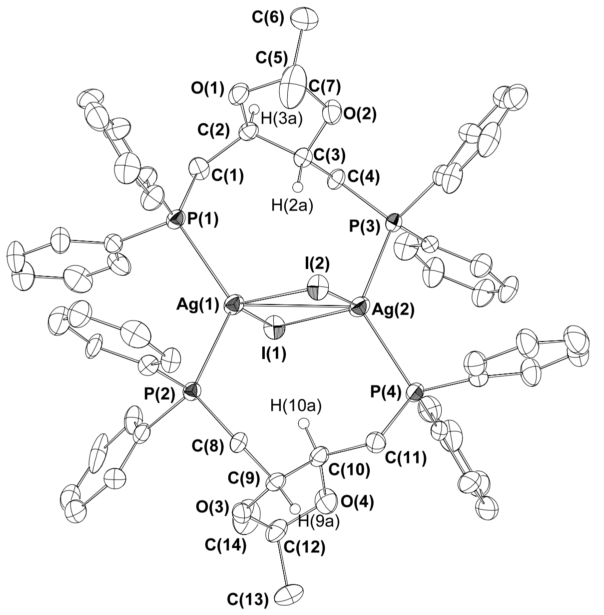

Fig. 3. Perspective view of [AgI(*R*,*R*-DIOP)]$_2$ at the 30% probability level.

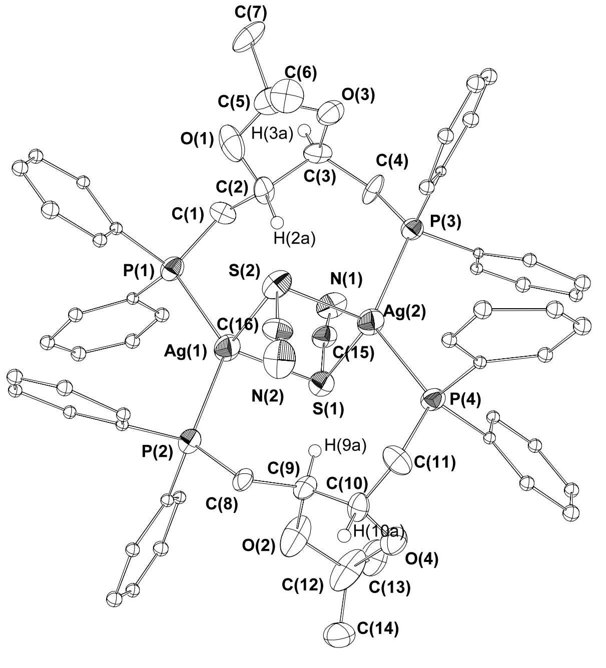

Fig. 4. Perspective view of [AgSCN(*R*,*R*-DIOP)]$_2$ at the 30% probability level.

Ag(1)–Ag(2)–Ag(3)–Ag(4) −114.0°. One CH_2Cl_2 and two H_2O molecules are crystallized in this complex. The H_2O molecules perhaps originate from the ambient moisture. The selected bond lengths and angles for complex **2** are collected in Table 4. The angles of P(1)–Ag(1)–P(2) and P(3)–Ag(2)–P(4) are 126.05(11), 128.35(12) and 129.43(12), 131.55(12)°, respectively. The Ag–P bond distances are 2.419(4) and 2.497(3) Å. The Ag–Br distances vary from 2.732(2) to 2.818(2) Å (average 2.782(2) Å), which is somewhat longer than that of the corresponding data in $[AsPh_4]_2[Ag(2)Br(4)]$ (average 2.677(1) Å) [21].

The selected bond lengths and angles for complex **3** are given in Table 5. Similar to complex **1**, the angles P(1)–Ag(1)–P(2) and P(3)–Ag(2)–P(4) are 120.56(9) and 124.04(9)°, much larger than 119.87(7)° in $(AgIP_2S_2C_{28}H_{28})_2$ [22]. The Ag–I bond lengths are 2.8959(9)–2.9877(11) Å in complex **3**, which is longer than those in $(AgIP_2SC_{28}H_{28})_2$ [23] (2.895(1) Å).

Table 3
Selected bond lengths (Å) and bond angles (°) for [AgCl(*R*,*R*-DIOP)]$_2$·2CHCl$_3$

Bond lengths			
Ag(1)–P(1)	2.472(4)	Ag(2)–P(3)	2.427(4)
Ag(1)–P(2)	2.490(5)	Ag(2)–P(4)	2.436(4)
Ag(1)–Cl(1)	2.649(4)	Ag(2)–Cl(2)	2.683(4)
Ag(1)–Cl(2)	2.674(4)	Ag(2)–Cl(1)	2.703(4)
Ag(1)···Ag(2)	3.724(1)	Cl(1)···Cl(2)	3.847(3)
Bond angles			
P(1)–Ag(1)–P(2)	130.71(14)	P(3)–Ag(2)–P(4)	133.61(14)
P(1)–Ag(1)–Cl(1)	97.22(14)	P(3)–Ag(2)–Cl(2)	117.77(13)
P(2)–Ag(1)–Cl(1)	118.83(14)	P(4)–Ag(2)–Cl(2)	96.75(14)
P(1)–Ag(1)–Cl(2)	117.67(14)	P(3)–Ag(2)–Cl(1)	94.37(14)
P(2)–Ag(1)–Cl(2)	94.53(14)	P(4)–Ag(2)–Cl(1)	116.15(15)
Cl(1)–Ag(1)–Cl(2)	92.55(13)	Cl(2)–Ag(2)–Cl(1)	91.18(13)
Ag(1)–Cl(1)–Ag(2)	88.18(12)	Ag(1)–Cl(2)–Ag(2)	88.09(12)

Table 4
Selected bond lengths (Å) and bond angles (°) for {[AgBr(*R*,*R*-DIOP)]$_2$}$_2$·CH$_2$Cl$_2$·2H$_2$O

Bond lengths			
Ag(1)–P(1)	2.473(3)	Ag(3)–P(6)	2.491(3)
Ag(1)–P(2)	2.481(3)	Ag(3)–P(5)	2.497(3)
Ag(1)–Br(2)	2.732(2)	Ag(3)–Br(3)	2.774(2)
Ag(1)–Br(1)	2.789(2)	Ag(3)–Br(4)	2.776(2)
Ag(2)–P(4)	2.419(4)	Ag(4)–P(8)	2.432(4)
Ag(2)–P(3)	2.421(4)	Ag(4)–P(7)	2.436(3)
Ag(2)–Br(1)	2.781(2)	Ag(4)–Br(4)	2.796(2)
Ag(2)–Br(2)	2.792(2)	Ag(4)–Br(3)	2.818(2)
Ag(1)···Ag(2)	3.547(1)	Ag(3)···Ag(4)	3.624(1)
Br(1)···Br(2)	4.264(1)	Br(3)···Br(4)	4.245(2)
Bond angles			
P(1)–Ag(1)–P(2)	126.05(11)	P(6)–Ag(3)–P(5)	128.35(12)
P(1)–Ag(1)–Br(2)	115.28(9)	P(6)–Ag(3)–Br(3)	98.99(9)
P(2)–Ag(1)–Br(2)	99.72(9)	P(5)–Ag(3)–Br(3)	114.11(9)
P(1)–Ag(1)–Br(1)	95.69(8)	P(6)–Ag(3)–Br(4)	115.01(9)
P(2)–Ag(1)–Br(1)	117.18(9)	P(5)–Ag(3)–Br(4)	97.74(9)
Br(2)–Ag(1)–Br(1)	101.09(5)	Br(3)–Ag(3)–Br(4)	99.80(5)
P(4)–Ag(2)–P(3)	129.43(12)	P(8)–Ag(4)–P(7)	131.55(12)
P(4)–Ag(2)–Br(1)	116.75(11)	P(8)–Ag(4)– Br(4)	114.09(9)
P(3)–Ag(2)–Br(1)	97.98(9)	P(7)–Ag(4)–Br(4)	98.08(8)
P(4)–Ag(2)–Br(2)	97.35(9)	P(8)–Ag(4)–Br(3)	96.24(10)
P(3)–Ag(2)–Br(2)	112.35(9)	P(7)–Ag(4)–Br(3)	114.61(9)
Br(1)–Ag(2)–Br(2)	99.82(5)	Br(4)–Ag(4)–Br(3)	98.24(5)
Ag(2)–Br(1)–Ag(1)	79.11(5)	Ag(3)–Br(3)–Ag(4)	80.80(5)
Ag(1)–Br(2)–Ag(2)	79.89(5)	Ag(3)–Br(4)–Ag(4)	81.16(5)

Table 5
Selected bond lengths (Å) and bond angles (°) for $[AgI(R,R\text{-DIOP})]_2$

Bond lengths			
I(1)–Ag(1)	2.8960(8)	I(1)–Ag(2)	2.9876(10)
I(2)–Ag(1)	2.9369(9)	I(2)–Ag(2)	2.9049(9)
Ag(1)–P(1)	2.503(2)	Ag(2)–P(3)	2.445(2)
Ag(1)–P(2)	2.508(2)	Ag(2)–P(4)	2.460(2)
Ag(1)–Ag(2)	3.0650(6)	I(1)···I(2)	4.9967(6)
Bond angles			
Ag(1)–I(1)–Ag(2)	62.77(2)	Ag(2)–I(2)–Ag(1)	63.29(2)
P(1)–Ag(1)–P(2)	120.58(8)	P(3)–Ag(2)–P(4)	124.03(8)
P(1)–Ag(1)–I(1)	102.20(6)	P(3)–Ag(2)–I(2)	112.70(6)
P(2)–Ag(1)–I(1)	111.34(6)	P(4)–Ag(2)–I(2)	101.96(7)
P(1)–Ag(1)–I(2)	111.74(7)	P(3)–Ag(2)–I(1)	94.53(6)
P(2)–Ag(1)–I(2)	94.10(6)	P(4)–Ag(2)–I(1)	108.34(7)
I(1)–Ag(1)–I(2)	117.88(3)	I(2)–Ag(2)–I(1)	115.98(3)

Table 6
Selected bond lengths (Å) and bond angles (°) for $[AgSCN(R,R\text{-DIOP})]_2$

Bond lengths			
Ag(1)–P(2)	2.436(7)	Ag(2)–P(4)	2.488(6)
Ag(1)–P(1)	2.452(6)	Ag(2)–P(3)	2.498(7)
Ag(1)–S(1)	2.687(6)	Ag(2)–S(2)	2.706(7)
Ag(1)–S(2)	2.824(9)	Ag(2)–S(1)	2.742(7)
Ag(1)–Ag(2)	3.307(2)	S(1)···S(2)	4.364(6)
Bond angles			
P(2)–Ag(1)–P(1)	129.3(2)	P(4)–Ag(2)–P(3)	124.3(2)
P(2)–Ag(1)–S(1)	103.6(2)	P(4)–Ag(2)–S(2)	109.6(2)
P(1)–Ag(1)–S(1)	112.1(2)	P(3)–Ag(2)–S(2)	105.7(2)
P(2)–Ag(1)–S(2)	102.6(2)	P(4)–Ag(2)–S(1)	104.2(2)
P(1)–Ag(1)–S(2)	101.7(2)	P(3)–Ag(2)–S(1)	105.1(2)
S(1)–Ag(1)–S(2)	104.9(2)	S(2)–Ag(2)–S(1)	106.6(3)
Ag(1)–S(1)–Ag(2)	75.0(2)	Ag(2)–S(2)–Ag(1)	73.4(2)

Table 7
The important mean bond lengths (Å) and bond angles (°) of complexes **1**–**4**

	1	**2**	**3**	**4**
Bond lengths				
Ag–P	2.456(4)	2.456(3)	2.479(2)	2.468(6)
Ag–X	2.677(4)	2.782(2)	2.9314(9)	2.740(7)
Ag–Ag	3.724(1)	3.586(1)	3.0650(6)	3.307(2)
Bond angles				
P–Ag–P	132.16(14)	128.84(12)	122.30(8)	126.8(2)
X–Ag–X	91.86(13)	99.74(5)	116.93(3)	105.8(2)

Table 6 shows the selected bond lengths and angles for complex **4**. The angles of P(1)–Ag(1)–P(2) and P(3)–Ag(2)–P(4) are 129.3(2) and 124.3(2)°, with Ag–P bond distances 2.436(7)–2.498(7) Å. Each thiocyanate is coordinated to two metals through a single S atom, differing from that in Ag(SCN)(PPr_3) [23], which contains a 1,1,3-μ^3-bonded SCN ligand. The average Ag–S distance (2.740(7) Å) is larger than that in molecular AgSCN (2.648(2) Å) [24].

The structures of the title complexes demonstrate the asymmetry of these molecules. The selected mean bond distances and angles of the cores of the complexes are given in Table 7. In these complexes, the values of the core diagonals (Å) are Ag···Ag = 3.724 (**1**), 3.586(1) (average) (**2**), 3.0651(6) (**3**), 3.307(2) (**4**), and X···X = 3.847 (**1**), 4.264(2) (average) (**2**), 4.9967(6) (**3**), 4.364(6) (**4**), respectively, i.e. the Ag···Ag distance(s) in the rhomboid of the core increases in the order of $I < S < Br < Cl$. Although it is not yet clear, these results may be partly helpful in explaining the tendency of the CD spectra. Additionally, the mean angle of P–Ag–P increases in the same order, from complex **3**, **4**, **2** to **1**, while that of X···Ag···X decreases in the same sequence. It should be interpreted as being due to the polarizability and electron distribution of the silver atom of the four ions as this decreases in the same order.

Acknowledgements

The research was supported by a grant from the state key laboratory of Structural Chemistry and the 'One-hundred Talents' program of the Chinese Academy of Sciences.

References

[1] T.P. Dang, H.B. Kagan, J. Chem. Soc. Chem. Commun. (1971) 481.

[2] (a) D. Heller, H. Buschmann, H.-D. Scharf, Angew. Chem. Int. Ed. Engl. 35 (1996) 1852;
(b) H. Brunner, L. Wagenhuber, J. Organomet. Chem. 525 (1996) 259 (and references therein).

[3] K. Prokai-Tatrai, S. Toros, B. Heil, J. Organomet. Chem. 315 (1986) 231.

[4] (a) A. Tillack, R. Selke, C. Fischer, D. Bilda, K. Kortus, J. Organomet. Chem. 518 (1996) 79;
(b) J. Vicente, J. Abad, J. Gil-Rubio, Organometallics 15 (1996) 3509;
(c) P. Salvadori, P. Pertici, F. Marchetti, R. Lazzaroni, G. Vitulli, M.A. Bennett, J. Organomet. Chem. 370 (1989) 155.

[5] (a) V. Gramlich, G. Consiglio, Helv. Chim. Acta 4 (1979) 105;
(b) S. Brunie, J. Mazan, N. Langois, H.B. Kangan, J. Organomet. Chem. 114 (1976) 225.

[6] J.M. Townsend, J.F. Blount, R.C. Sun, S. Zawoiski, D. Valentine Jr., J. Org. Chem. 45 (1980) 2995.

[7] (a) J.-M. Lehn, Comprehensive Supramolecular Chemistry, Pergamon, Oxford, 1996;
(b) M.J. Zaworotko, Chem. Soc. Rev. 24 (1994) 283.

[8] A.J. Blake, N.R. Champness, S.S.M. Chung, W.-S. Li, M. Schröder, J. Chem. Soc. Chem. Commun. (1997) 1005.

[9] (a) F. Caruso, M. Camalli, H. Rimml, L.M. Venanzi, Inorg. Chem. 34 (1995) 673;
(b) S. Kitagawa, M. Kondo, S. Kawato, S. Wada, M. Mackawa, M. Munakata, Inorg. Chem. 34 (1995) 1455.

[10] (a) S.J. Berners-Price, R.K. Johnson, A.J. Giovenella, L.F. Faucette, C.K. Mirabelli, P.J. Sadler, J. Inorg. Biochem. 33 (1988) 285;

(b) S.J. Berners-Price, P.J. Sadler, Coord. Chem. Rev. 151 (1996) 1.

[11] C. Che, H. Yip, D. Li, S. Peng, G. Lee, Y. Wang, S. Liu, J. Chem. Soc. Chem. Commun. (1991) 1615.

[12] A. Yanagisawa, H. Kageyama, Y. Nakatsuka, K. Asakawa, Y. Matsumoto, H. Yamamoto, Angew. Chem. Int. Ed. Engl. 38 (1999) 3701.

[13] B. Wu, W.J. Zhang, S.Y. Yu, X.T. Wu, J. Chem. Soc. Dalton Trans. (1997) 1795.

[14] B.A. Murrer, J.M. Brown, P.A. Chaloner, P.N. Nicholson, D. Parrer, Synthesis (1979) 350.

[15] SHELXL-93, Software Reference Manual, Siemens Energy & Automatic Inc.

[16] H.D. Flack, Acta Crystallogr. A 39 (1983) 876.

[17] P. Gans, J.B. Gill, D.P. Fearnley, J. Chem. Soc. Dalton Trans. (1981) 1708.

[18] K. Nilsson, A. Oskarsson, Acta Chem. Scand. Ser. A 36 (1982) 605.

[19] A. Cassel, Acta Crystallogr. B 32 (1976) 2521.

[20] A. Cassel, Acta Crystallogr. B 35 (1979) 174.

[21] G. Helgesson, S. Jagner, J. Chem. Soc. Dalton Trans. (1990) 2413.

[22] A. Cassel, Acta Crystallogr. B 31 (1975) 1194.

[23] C. Panattoni, E. Frasson, Gazz. Chim. Ital. 93 (1963) 601.

[24] G. Wilkinson (Ed.), Comprehensive Coordination Chemistry, vol. 5, 1987, p. 795.